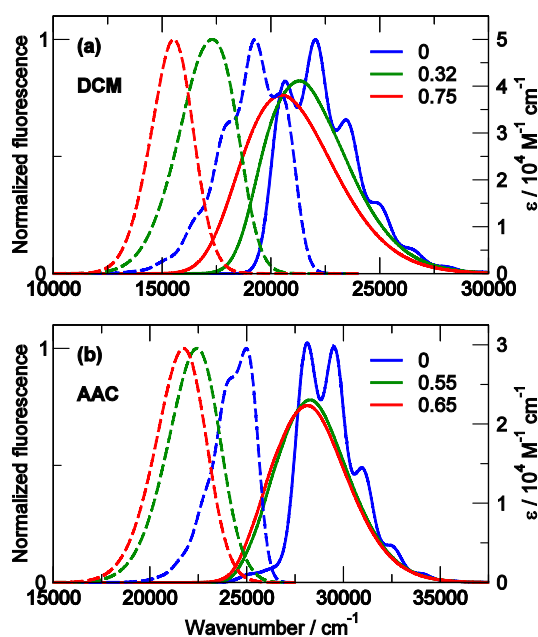


# Two-dimensional electronic-vibrational spectra: modeling correlated electronic and nuclear motion

Francesca Terenziani, and Anna Painelli

*Dipartimento di Chimica, Università di Parma & INSTM UdR Parma, Parco Area delle Scienze 17/a, 43124 Parma, Italy*

## Supporting Information



**Figure S1.** Panel a: Absorption spectra (full lines) and fluorescence spectra (dashed lines) calculated for DCM based on the two-state model (parameters in Table S1) for solvents of increasing polarity (increasing  $\epsilon_{or}$ ) from hexane, to chloroform to DMSO. Panel b: Absorption spectra (full lines) and fluorescence spectra (dashed lines) calculated for AAC with a three-state LE/CT model (parameters in Ref. <sup>1</sup>) for solvents of increasing polarity (increasing  $\epsilon_{or}$  values) from cyclohexane, to methylene chloride to DMSO.

Absorption and fluorescence spectra of DCM\* show a prominent solvatochromism, with substantial red shifts in polar solvents and an intriguing evolution of the bandshapes. The well-pronounced variation of the fluorescence spectrum, showing a well-resolved vibronic structure in non-polar solvent and an unresolved but overall narrower shape in polar solvents, is often taken as an evidence of a twisted intermolecular charge-transfer (TICT) state being populated in polar solvents after the vertical excitation to a locally-excited state. However, our two-state model describes very well the complex spectral behavior of DCM in different solvents without the need to introduce any TICT or LE state, but simply accounting for the inherent polarizability of the electronic system.<sup>2</sup> The possibility to quantitatively reproduce the spectral behavior of DCM based on the two-state model does not demonstrate the absence of a LE/TICT interplay, but proves at least that it is not required to explain optical spectra of DCM.

\* The spectra reported here for DCM (Figure S1, panel a) slightly differ from those published in Ref. <sup>2</sup>: in the original paper, in fact, the Hamiltonian was solved in the adiabatic approximation and the spectra were calculated in the harmonic approximation, while here the two approximations are fully relaxed. The differences are however minor: the adiabatic and harmonic approximations work well for push-pull dyes, while are untenable in the case of LE/CT interplay.

The absorption spectra of AAC (Figure S1, panel b) are characterized by an intense band located at 28.000-30.000  $\text{cm}^{-1}$  showing a pronounced solvatochromism and an important broadening in polar solvents. This band can be safely ascribed to a CT absorption polarized along the D–A axis. Two weaker absorption features (in the 25.000 and 26.000  $\text{cm}^{-1}$  region) are clearly seen in non-polar or weakly polar solvents. In polar solvents, the CT band moves to the red, overlapping these small features. These weak bands are assigned to a LE transition (with its own vibronic structure) involving the condensed rings. The fluorescence signal measured in non-polar solvents is ascribed to the emission from the LE state. However, the fluorescence acquires a CT character in polar solvents, as demonstrated by the prominent solvatochromism, the large Stokes shift, and the conspicuous inhomogeneous broadening. The CT state is in fact stabilized in polar solvents, lowering its energy below the LE state, as shown by the PES reported in Figure 2 of main text, right-bottom panel (relevant to DMSO). Absorption, fluorescence and fluorescence anisotropy spectra of AAC in different solvents are quantitatively reproduced by the three-state model as well,<sup>1</sup> a nontrivial result in view of the reduced number of model parameters.

**Table S1.** Molecular parameters of the essential-state model for DCM.

	$\eta$ [eV]	$\tau$ [eV]	$\omega_v$ [eV]	$\varepsilon_v$ [eV]	$\mu_0$ [D]	$\Gamma_{el}^{(a)}$ [eV]	$\Gamma_{vib}^{(b)}$ [eV]
<b>DCM</b>	1.14	0.88	0.172	0.456	28	0.08	0.001

<sup>(a)</sup> Homogeneous width (half width at half maximum) of the electronic transitions. <sup>(b)</sup> Homogeneous width (half width at half maximum) of the vibrational transitions

The model parameters used for DCM (Table S1) are the same as previously extracted,<sup>2</sup> with only a minor variation of the vibrational frequency ( $\omega_v$ ) and relaxation energy ( $\varepsilon_v$ ), as to better reproduce the main vibrational features of 2D-EV spectra. These small changes have negligible effects on the electronic spectra.

### Assignment of the bandwidths to the excited-state absorption transitions in AAC

In DCM the adiabatic approximation works well and excitations are easily classified as electronic or vibrational in nature, looking at the nature of the relevant eigenstates. Accordingly, we assign a bandwidth of 0.001 and 0.08 eV to vibrational and electronic transitions, respectively (see Table S1). In AAC, the situation is more delicate because, due to the large nonadiabatic mixing of LE and CT states, transitions cannot be simply classified as electronic or vibrational. In order to assign appropriate bandwidths to transitions in AAC, we calculate the LE and CT characters ( $l_i$  and  $c_i$ , respectively) of each excited state  $i$  (via the eigenvectors) and assign to each  $i \rightarrow j$  transition a bandwidth calculated as a combination of vibrational and electronic bandwidths:

$$\Gamma_{ij} = \frac{(l_i l_j + c_i c_j) \Gamma_{vib} + (l_i c_j + c_i l_j) \Gamma_{el}}{l_i l_j + c_i c_j + l_i c_j + c_i l_j}$$

In this way, if the transition occurs between two states having the same main character (no matter if LE or CT), the bandwidth is close to that expected for a vibrational transition; if the two involved states have opposite characters, the bandwidth assumes typical values for electronic transitions. The bandwidth is intermediate in all other cases, according to the respective LE and CT characters of the two involved states.

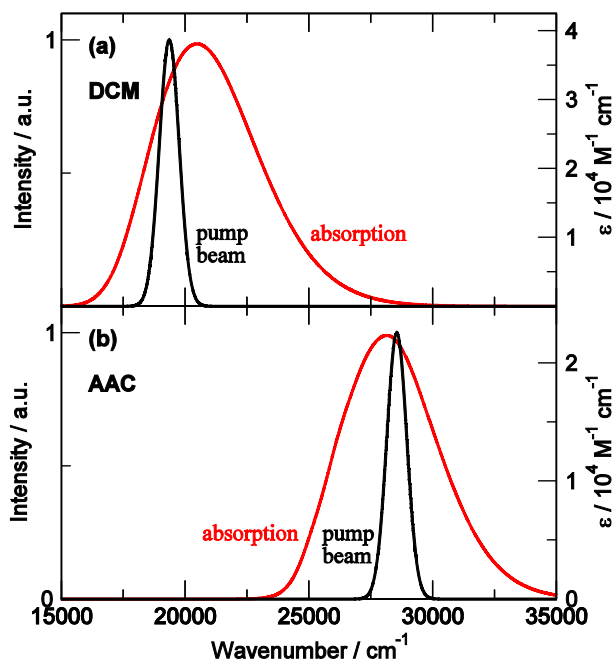


**Figure S2.** Spectral profiles of the pump beams used for the calculation of 2D-EV spectra, together with the absorption profiles of DCM and AAC in DMSO (panel a and b, respectively).

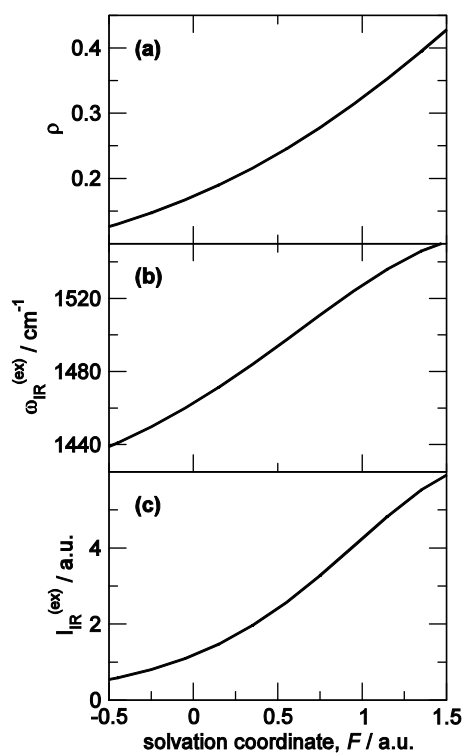


**Figure S3.** The amount of mixing between the diabatic basis states, expressed through the  $\rho$  parameter (panel a); the vibrational frequency and the vibrational transition intensity relevant to the electronic excited state (panel b and c, respectively) as functions of the solvation coordinate. Results obtained through the two-level model with the parameters relevant to DCM.

In the two-level model for push-pull dyes, the most convenient quantity to describe the electronic nature of the dye is  $\rho$  (univocally determined by the model parameters  $\eta$  and  $\tau$ ), that is the weight of the charge-separated basis state into the ground state, in other words the amount of charge transfer in ground state:  $D^{+p}-\pi-A^{-p}$ .<sup>3</sup> Due to the inherent polarizability of push-pull molecules, the electronic nature (represented by the  $\rho$  parameter) strongly depends on the interaction of the electronic system with other degrees of freedom,

including molecular vibrations and polar solvation. The interaction is typically self-consistent: not only vibrational and solvation degrees of freedom affect the electronic structure of the dye, but also the electronic structure of the dye affects vibrational coordinates and polar solvation. This means that whenever one of these coordinates changes, all the others are affected in a self-consistent way.

In particular, as the solvation coordinate spans different values (as due to disorder or increasing solvent polarity or solvation dynamics), the nature of the electronic states is affected, affecting in turn the vibrational properties. This behavior is sketched in Figure S3, where we show the dependence of electronic and vibrational properties on the solvation coordinate (case of DCM). Specifically, panel (a) reports the evolution of the  $\rho$  parameter, panels (b) and (c) show the evolution of the excited-state vibrational properties, namely the vibrational frequency and intensity, respectively. As the solvation coordinate moves to higher values, the two electronic states increase their mixing ( $\rho$  moves closer to 0.5) and the excited-state vibrational frequency hardens, as well as its IR absorption intensity increases.

These results, reported here for DCM parameters, are general: high values of the solvation coordinates always induce the  $\rho$  parameter to move closer to 0.5 (even in the case of  $\rho > 0.5$ ) and a consequent hardening and IR absorption intensity increase of the excited-state vibrational mode.

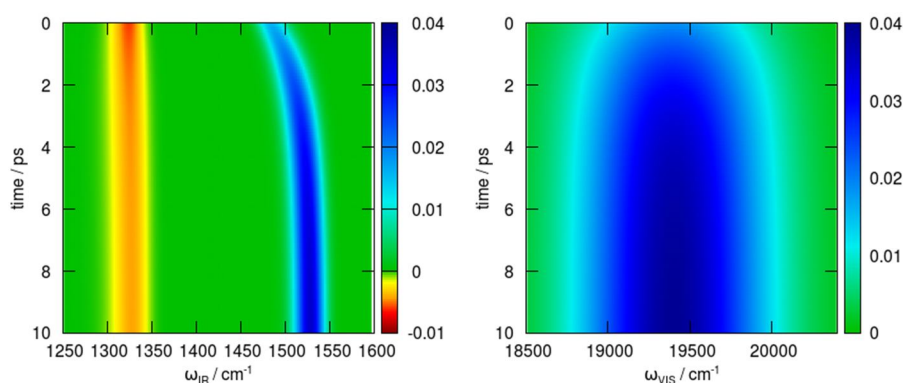


**Figure S4.** Left panel: Time evolution of the ground-state IR-absorption bleach band (negative  $\Delta A$ , red) and of the excited-state IR absorption band (positive  $\Delta A$ , blue) along the  $\omega_{\text{IR}}$  axis (integration of the corresponding 2D signals over  $\omega_{\text{VIS}}$ ). Right panel: Time evolution of the excited-state IR absorption band along the  $\omega_{\text{VIS}}$  axis (integration of the positive 2D signal over  $\omega_{\text{IR}}$ ). Both panels refer to DCM in DMSO (two-state model with parameters reported in Table S1).

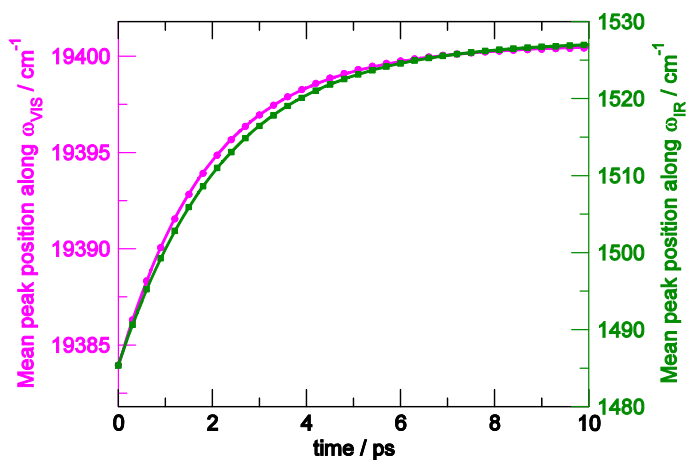


**Figure S5.** Calculated time evolution of the mean position of the excited-state IR absorption band along the  $\omega_{\text{VIS}}$  axis (magenta dots, left axis) and along the  $\omega_{\text{IR}}$  axis (green dots, right axis), referred to DCM in DMSO. Full lines show the corresponding monoexponential fits, characterized by time constants of 1.96 and 2.24 ps, respectively.

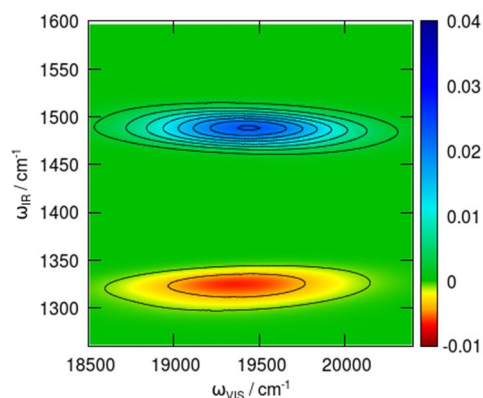


**Figure S6.** Purely absorptive 2D-EV spectrum calculated for DCM in DMSO via the two-state model (parameters in Table S1) at zero time after excitation, before vibrational cooling. The color map reports the  $\Delta A$  value according to the palette on the right (arbitrary units).

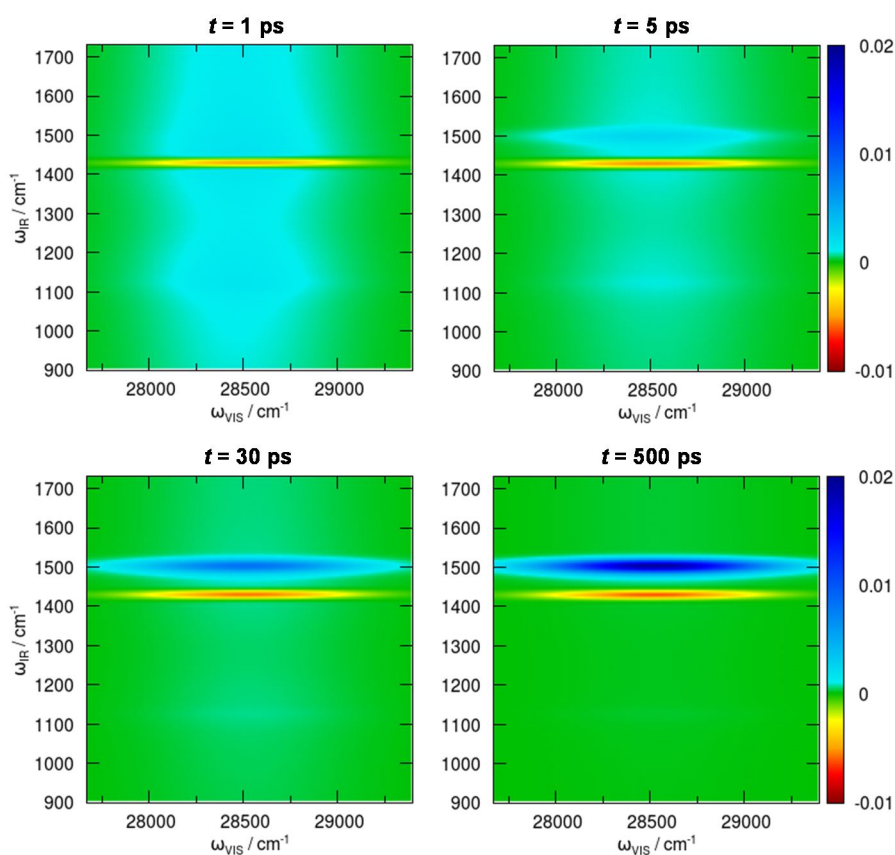


**Figure S7.** Purely absorptive 2D-EV spectra calculated for AAC in DMSO via the three-state LE/CT model (parameters in Ref. <sup>1</sup>), for the delay times reported on top of each panel. The color maps report the  $\Delta A$  value according to the palettes on the right (arbitrary units).

1. C. Sissa, V. Calabrese, M. Cavazzini, L. Grisanti, F. Terenziani, S. Quici, and A. Painelli, *Chem. Eur. J.*, 2013, **19**, 924–935.
2. B. Boldrini, E. Cavalli, A. Painelli, and F. Terenziani, *J. Phys. Chem. A*, 2002, **106**, 6286–6294.
3. A. Painelli and F. Terenziani, *Chem. Phys. Lett.*, 1999, **312**, 211–220.